The Theoretical and Experimental Investigation into Technological Parameters of High-Melting Metal Arc Spraying

C.H. Li*, S. Wang and Y.C. Ding

School of Mechanical Engineering, Qingdao Technological University, 266033 China

Abstract: The experimental study is done for technological parameters of high-melting metal arc spraying to study the influence of spraying current, spraying voltage and wire feed voltage on spraying arc and the influence of spraying current on coating temperature and analyze theoretically the distribution rules of spray gun jet speed field and temperature field and their influencing factors. The results showed that the arc current increases along with arc voltage increase. The lower the spraying voltage is, the smaller the molten grain size becomes. However, if the arc voltage is lower than the minimum critical arc voltage of the material, the arc could not keep smooth burning. The spraying current has correspondence relationship with wire feed speed. The spraying current could be adjusted through wire feed speed adjustment.

Keywords: High-melting metal arc spraying, technological parameters, spraying current, spraying voltage, coating temperature.

1. INTRODUCTION

In the ark spraying process, the wire feeder is used to send continuously and evenly two electric conduction wires into two current conduction nozzles in arc pistol with the current conduction nozzles connected to positive and negative poles of the power supply and insulated before junction of two wires. When tips of two wires mutually touch each other at the junction position of the nozzle, the short circuit is generated between two wires thus to produce arc [1]. After the wire tip is melted, the melted metal drop has been atomized and accelerated by compressed air to jet into surface of female die in a fast speed and combine with the machinery on the surface of female die to form arc spraying coating. The arc spraying principle is shown in Fig. (**1**).

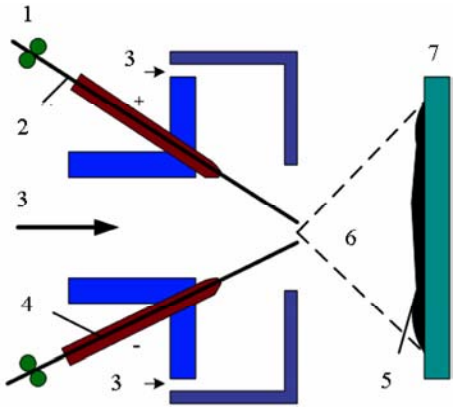

Fig. (1). The arc spraying principle. 1- wire feeder; 2- electric conduction wire; 3- compressed air; 4- nozzle; 5- spraying coating; 6- melted metal drop; 7- die surface.

*Address correspondence to this author at the School of Mechanical Engineering, Qingdao Technological University, 266033 China;
Tel: +86-532-85071757; Fax: +86-532-85071286;
E-mail: sy_lichanghe@163.com

The rapid moulding technology of metal arc spraying is a ”reproduction” moulding technology thatwith physical model (or called prototype) as female die and arc as heat source [2], the melting metal materials are atomized with high speed airflow to form spraying grains, which are made to jet and deposit on the surface of female die to form compact metal coating in fixed thickness, known as die shell. Since the die shell accurately copies the prototypical shape and gets the necessary die cavity, the die’s rapid manufacture is completed after reinforcement, demoulding, polishing and other post-processing technology [3]. The process flow of metal arc spraying moulding is shown in Fig. (**2**), mainly including: female die preparation; female die surface pretreatment; metal arc spraying; filling lining materials; demoulding and post-processing, etc. As a matter of fact, metal arc spraying rapid moulding technology is near net-shape rapid moulding technology [4]. The arc spraying mould making usually does not require for additional mechanical processing after accomplishment and, could be directly used for shaping manufacture. The numerical control finish machining for a little cutting output is required according to actual situation and demand to obtain higher shape precision, size precision and surface quality [5-8].

Metal arc spraying moulding technology takes female die as the standard that the die cavity size and geometric precision are completely from female die. Since cavity surface and its fine figure are formed at the same time, so it features in fast moulding speed, short moulding cycle, low cost and longer service life for the die. The processing cycle is 1/3-1/10 of the traditional steel die numerical control and the expense is 1/3-1/5 or lower, which becomes an important way for new product development and small lot production. Presently, this rapid moulding technology has been widely applied to airplane, automobile, appliance, furniture, shoemaking, art-ware and other industries. In various injected shaped dies with complicated surface shapes and fine figures, the characteristic details for figure duplication could be 5μm. The deformation in a whole is very small

1874-088X/12 2012 Bentham Open

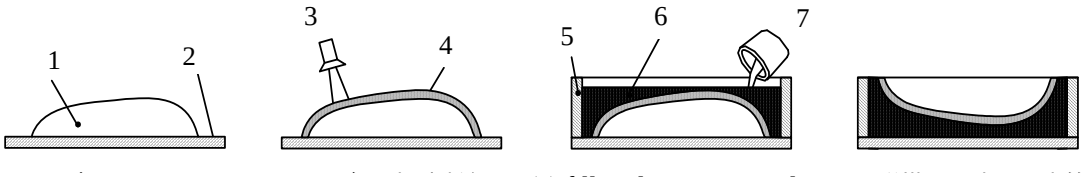

(a) die pretreatment (b) arc spraying (c) filling lining materials (d) demoulding and after-treatment

1- female die; 2- motherboard; 3- spraying gun; 4- metal coating; 5- frame; 6- lining material; 7- filling vessel

Fig. (2). The process flow chart of metal arc spraying moulding.

since the material's phase change partition is occurred in spraying complex and phase change transformation could be made up from the neighboring area, which is different from the casting process that its transformation is big for its overall phase change [9-11].

The middle and low melting metal arc spraying rapid moulding technology represented with zinc or zincaluminium alloy, etc has been applied in die development and sample automobile manufacture of large automobile panel, showing huge technological value and good economic benefit upon its fast and low cost features. However, since the hardness of zinc and zinc aluminium alloy is relatively low, the die's service life and application scope is restricted to certain extent. It is extremely attractive to manufacture arc spraying die with high melting point and high hardness metal (carbon steel and alloy steel) not only because the material is relatively cheap but also the die shell with high hardness and strength could greatly improves the service life of spraying die thus to expand the application scope of spraying die to provide better service for forming manufacture industry [12]. However. the high melting point metal has bigger coating contractibility rate, thermal stress and porosity in spraying and the coating is easy for cracking, warping or spalling, making it diffidult to manufacture die shell and hard to control technological parameters. Theoretical analysis and experimental research have been done for high melting point metal arc spraying technological parameters in this paper.

2. THE INFLUENCE OF SPRAYING TECHNOLOGICAL PARAMETERS ON COATING ORGANIZATION AND MECHANICAL PROPERTY

The speed and temperature of molten drop are two important factors to influence on internal stress of arc coating. To analyze for spray gun's jet speed field and temperature field, master spraying mechanism and the deposition process of spraying grain have significant effect to reduce coating internal stress, control spraying coating quality and improve spray moulding technology level. Spraying current and spraying voltage control output power of power source, known as arc combustion power; wire feed voltage determines wire feed speed, known as wire quantity to be melted by the arc in unit time; the compressed air has cooling effect while atomizing metal molten drop, so spraying current, spraying voltage, wire feed voltage, air pressure and flow will impact on the temperature of metal grain. Air jet flow speed determines the flying speed of grains that grains in flying under the effect of compressed airflow have severe changes along with different temperatures and speeds of spraying distance. When reaching at matrix surface, the grain's speed and temperature determine coating stress and coating quality. Grain's flying speed could be as fast as possible to increase grain's pressure stress generated in striking to balance part coating tensile stress, which is beneficial to increase coating's critical thickness. If the temperature is too low, the solid phase proportion in the grains is high that grain is easy to rebound and reduce deposit efficiency [13]; if the temperature is too high, liquid phase proportion is increased that the grain is easy to splash and the coating is in poor quality. Table **1** shows melting values of commonly used spraying materials. Seen from Table **1**, the melting point of 3Cr13 is over 1000°C, belonged to martensite stainless steel high-melting metal material that the coating has features of high bond strength, low contractibility rate, low residual stress and good abradability, etc.

Table 1. Melting Values of Commonly Used Spraying Materials

Materials	Melting Values (°C)
Zn	419.5
Al	660.4
ZnAl15	677
Cu	1083
3Cr13	1482

Since the metal liquid drop size and diameter distribution are related to technological parameters such as fuse voltage, wire feed speed and atomization gas pressure, etc and the average temperature of metal jet flow is related to spraying distance, the combined method of experiment analysis and numerical calculation is used to build the relationship between spraying technological parameters and coating quality.

3. THE RELATIONSHIP AMONG SPRAYING VOLTAGE, WIRE FEED VOLTAGE AND SPRAYING CURRENT

QD8-LA arc spraying system and 3Cr13 martensite stainless steel wire with spraying diameter ofφ2 are used to study in the experiment for the influence of spraying voltage and wire feed voltage on spraying current.

3.1. The Experimental Results

The experimental result is shown in Table **2**. Under the precondition of unchanged wire feed speed, the arc current is in increase tendency when the arc voltage is increased from

27V to 40V, When the arc electric intensity E is unchanged, arc column length d=U/E, increase arc voltage U, elongate the arc column. the arc section can not magnify along with current increase proportionally thus to speed up heat loss of the arc column [14]. In order to balance the loss, the power source must provide more heat energy (IE). When E is unchanged, the current (I) becomes bigger.

Table 2. Spraying Current Values

Voltage (V) / Current (A) / Voltage (V)	9	10	12	14	15
27	100	120	150	190	200
30	100	120	150	190	210
33	110	130	160	190	210
35	110	120	180	210	220
40	110	140	190	230	240

Since the arc voltage reflects space among wire tips, to effectively control arc voltage could maintain geometrical shape stable in atomization area [15]. Each material has the minimum arc voltage value to maintain the arc smooth burning. The lower the spraying voltage is, the smaller the molten grain size becomes. However, if the arc voltage is lower than the minimum critical arc voltage of the material, the arc could not keep smooth burning. When the spraying voltage is higher than the critical arc voltage, the gap among wire tips, spraying jet angle and particle size of spraying grains will magnify along with voltage increase as well asthe burning loss of the sprayed materials. In particular, those elements easily compounded with oxygen have more serious burning loss [16]. The deposit efficiency will gradually reduce along with increase of spraying voltage. Seen from that, the arc voltage has great influence on spraying quality. Under the precondition to guarantee smooth burning of arc, the spraying voltage value should be chosen as low as possible, thus, the spraying 3Cr13 voltage is confirmed to be 30V in this experiment.

The influence of wire weed voltage on arc current is shown in Figs. (**3**, **4**). From Fig. (**4**), it can be seen that in the magnifying process for the wire feed voltage from 9V to 15V, the arc current gradually increases. It is found that the influence of wire feed speed is more obvious on arc current than on spraying voltage by comparing Fig. (**3**) and Fig. (**4**). Under the precondition of unchanged arc voltage, to increase wire feed voltage speeds up spraying wire feed speed and to melt metall wire consumes more arc heat. In order to balance the loss, the power source must provide more heat energy and the current I becomes bigger. Under the effect of arc and atomization airflow, the tips of two metal wires undergo frequently the process of metal melting-molten metal breaks away-molten drop atomized into particles. In each process, the distance between two poles is frequently changed. When the voltage of power resource keeps constant, for current's self-adjusting feature, the arc current has frequent fluctuations accordingly. When the arc length becomes smaller, the current could rapidly magnify to speed up wire's melting and recover the arc length. When the arc length becomes bigger, the current also rapidly decreases to reduce wire's melting speed and recover the arc length, so that the current could self-maintain wire's melting speed.

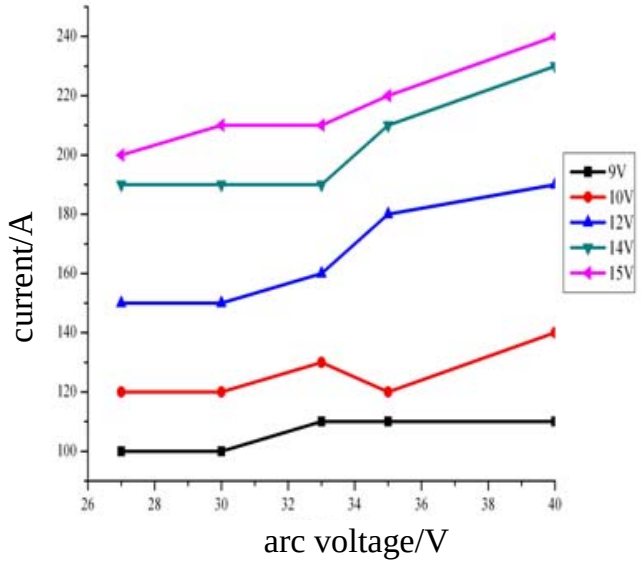

Fig. (3). The influence of arc voltage on arc current.

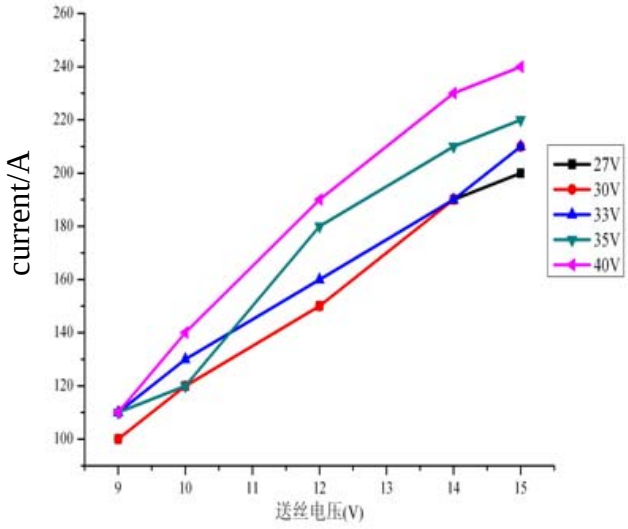

Fig. (4). The influence of wire weed voltage on arc current.

It is noted that when the spraying voltage is unchanged, the spraying current has corresponding relationship with wire feed speed rather than with wire feed voltage. When the wire feed speed is the same, if the resistance of the wire feed system is changed, the wire feed voltage must also be adjusted. In the experiment, the wire feed voltage is adjusted according to spraying current value.

4. THE EFFECT OF SPRAYING CURRENT ON COATING TEMPERATURE

The spraying current determines spraying efficiency and the arc temperature. If the spraying current is different, the temperature of metal particles is surely different, so is the

temperature of spraying coating. The coating temperature is the key factor to cause coating internal stress.

Firstly prepare 100×100×20mm cast iron matrix. The infrared radiation thermometer is used to real-time monitor in the spraying process temperature changes at single point on the coating surface. QD8-LA arc spraying system is adopted to spray 3Cr13 martensite stainless wire with spraying diameter ofφ2 and the spraying technological parameters are shown in Table **3**. For matrixes with different initial temperatures, the coating temperatures are also various and the coating temperature will increase along with increase of the initial temperature. Therefore, the coating needs to be cooled to 20°C before each spraying in the experiment to achieve the comparability. The spraying current sprays the coating in every 20A from 100 A to 180A. Since the temperature fluctuation is great, choose five repeated samples for each current value to detect the coating temperature in each spraying process and take the average value as the final result.

Table 3. Spraying Technological Parameters of 3Cr13 Material

Arc Voltage (V)	Spraying Distance (mm)	Spraying Pressure (MPa)	Jet Flow (m^3/min)
30	260	0.5	2.4

5. THE EXPERIMENTAL RESULTS AND ANALYSIS

The experiment result is shown in Table **4**. Seen from Fig. (**5**), when the current increases from 100A to 180A, the highest temperature on the coating surface is in increase tendency. Under the condition in this experiment, taking 20°C as the initial temperature, the change amplitude is 38.41°C when the highest temperature increases from 82.24°C to 120.65°C. In order to reduce spraying coating temperature, under the precondition to guarantee smooth jet flow, the wire feed speed should be as low as possible thus to reduce spraying current. In the deposition process for each layer, the temperature fluctuation occurs at any point on the coating surface along with shift of jet flow light spot, equally to bear thermal shock cyclic loading effect. The temperature change each time accompanies with the change of coating internal stress. According to result of this experiment, it is primarily to choose the spraying current of 100A, the initial temperature of 20°C, the temperature fluctuation range of 62.3°C in the spraying process and the highest temperature of 82.24°C.

Table 4. The Effect of Spraying Current on Coating Temperature

Spraying current (A)	100	120	140	160	180
Maximal temperature (°C)	82.24	88.73	101.02	112.92	120.65
Minimal temperature (°C)	19.95	20.03	19.87	20.26	20.85
Temperature fluctuation (°C)	62.28	68.7	79.43	92.66	101.63

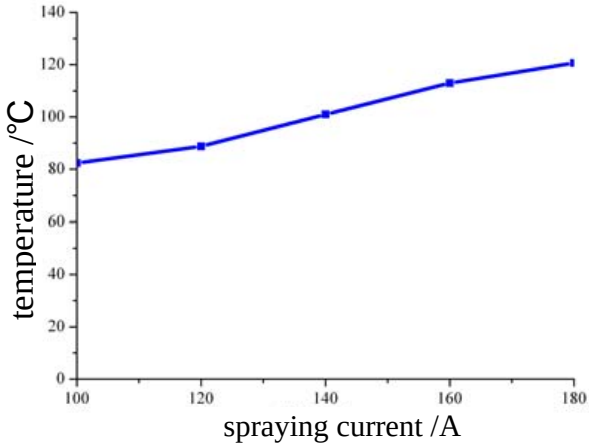

Fig. (5). The effect of spraying current on coating temperature.

6. NUMERICAL SIMULATION AND EXPERIMENTAL ANALYSIS SPEED FIELD AND TEMPERATURE FIELD OF AIRFLOW

The grain deposition process is divided into two stages: in the first stage, the mutual effect of metal drop with airflow in flying process; the second stage, the metal drop collides with matrix to freeze and deposit. In the first stage, the metal drop produced by high pressure airflow atomization speeds up to fly towards matrix under high pressure and airflow effect and cool in the high pressure airflow. According to different metal drop and cooling speed, the metal particles are existed in complete liquid, semi-solid and solid states before striking the matrix. The proportions of metal particles in various states determine the average temperature of metal jet flow. Since the grain's flying time is only 1ms with fast flying speed and rapid temperature change together with the bad condition around jet flow, it is hard to directly detect jet flow state with experimental devices. The research method is mainly numerical calculation and simulation analysis. The change process between high speed flying grain speed and temperature in the jet flow has been quantitatively analyzed with the combined method of FLUENT numerical simulation and experimental analysis.

7. NUMERICAL SIMULATION OF FLOW FIELD

7.1. Flow Field Modeling, Gridding Division and Continuous Phase Loading

Since the spray gun and its jet flow are axial symmetry structure, in order to simplify the calculation, the current conduction nozzle in the spray gun is ignored. The triangle gridding is adopted for division, the boundary conditions are: inlet pressure 0.5MPa, outlet pressure 0MPa and the initial pressures of up and down wall surfaces in jet flow area 0MPa.

The sprayer nozzle increases air velocity by changing section's geometric dimension in a short route. In the sprayer nozzle firstly contracted and then magnified, the subsonic velocity airflow speeds up in the reducing pipe; the sound velocity appears at the minimum section, which is accelerated to be supersonic speed after entering into increasing coupling. It is assumed that the air is the ideal gas,

meaning gas's viscosity is not considered. The airflow is isentropic, zero friction and heat insulation that it flows in straight line from the inlet to the outlet. The gas has compressibility.

According to gas jet dynamics principle, the speed of compressed jet flow at the outlet could be calculated with the following formula [17]:

$$V_e = \sqrt{\frac{TR}{M} \cdot \frac{2k}{k-1} \cdot \left[1-\left(P_e/P\right)^{(k-1)/k}\right]} \quad (1)$$

In the formula:

α_c =exhaust velocity at outlet of sprayer nozzle, m/s;

α_s =thermodynamics temperature of the air at inlet, K;

R =common air constant, (8314.5 J/(kmol•K);

M =air molecule quality, kg/kmol;

k =cp/cv=adiabatic index;

cp=air specific heat at constant voltage;

cv=air specific heat at constant volume;

P_e =air absolute pressure at outlet, Pa;

P = air absolute pressure at inlet, Pa;

The Figs. (**6**, **7**) are the velocity change of airflow axial along with axial distance. Seen Fig. (**6**) and Fig. (**7**) for simulation result, at the spray gun outlet, the highest air speed reaches 600m/s with violent disturbance wave. After ejection, the air velocity rapidly reduces to subsonic velocity

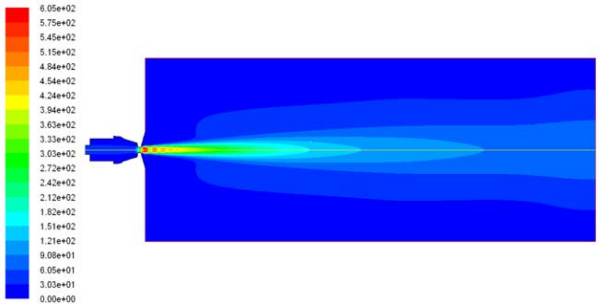

Fig. (6). Velocity field nephogram of melted metal airflow.

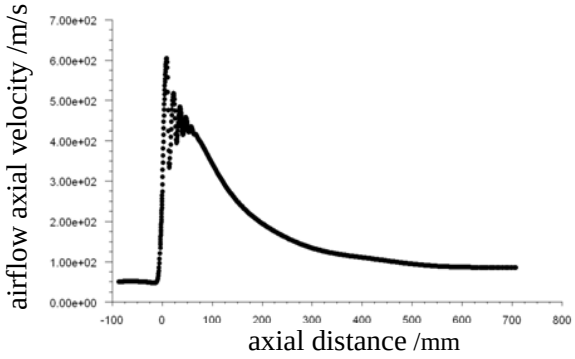

Fig. (7). The change of airflow axial velocity along with axial distance.

(about 200m/s) within the spraying distance of 0-250mm. The air velocity continuously decreases along with greater of spraying distance. The high speed air atomizes metal molten drop, drives metal drop to accelerate flying towards the matrix and meanwhile quickly cools the high temperature molten drop.

7.2. The Load Result of Dispersed Phase

Based on continuous phase analysis, load dispersed phase and conduct secondary calculation. Table **5** is dispersed phase parameter. The boundary conditions are: initial temperature 3000K, initial speed 0m/s, particle diameter 25μm and flow 0.00139kg/s. The loaded result of dispersed phase is shown in Figs. (**8**, **9**).

Table 5. Dispersed Phase Parameters of 3Cr13 Material

Items	Values
melting point (°C)	1482
boiling point (°C)	300s
density (kg/m^3)	7.89e3
specific heat capacity (J/kg·K)	460
thermal conductivity (W/m·k)	24.9

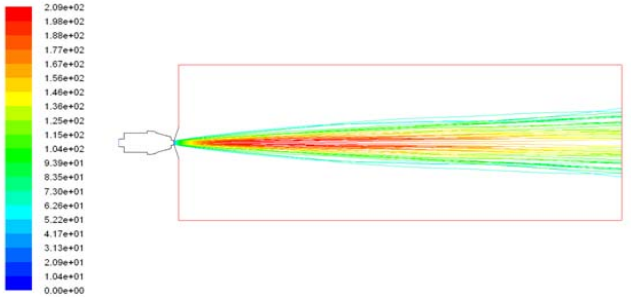

Fig. (8). Velocity distribution nephogram of melted metal airflow.

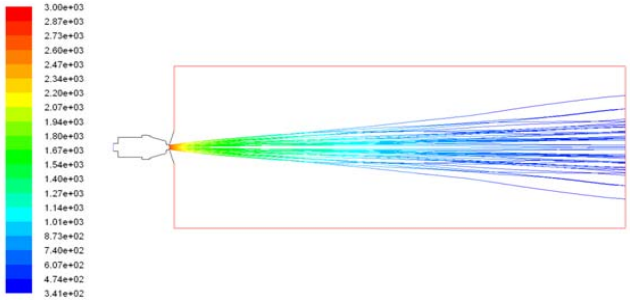

Fig. (9). Temperature distribution nephogram of melted metal airflow.

According to aerodymanics principle, the change of gas axial velocity along with axial distance x is represented as:

$$V_g = V_{gi} \exp\left(-\frac{x}{\lambda}\right) \quad (2)$$

In the formula, V_{gi} is air speed at the outlet and λ is the attenuation coefficient (0.1～0.3).

The total acting force F received by spherical metal drop with diameter of d is represented with the following formula:

$$F = m\left(dV_d/dt\right) = C_D\rho_g\left(V_g\text{-}V_d\right)^2 \cdot A/2 \quad (3)$$

A is sectional area of metal drop.

The accelerated speed of metal drop [19]:

$$dV_d/dt = 3C_D\rho_g\left(V_g - V_d\right)\left|V_g - V_d\right|/4d\rho_d \quad (4)$$

The drag coefficient C_D is related to Reynolds number.

$$C_D = 0.28 + \left[6/\mathrm{Re}\right]^{1/2} + \left[21/\mathrm{Re}\right] \quad (5)$$

The effect of different air pressures on airflow velocity can be shown in the Fig. (**10**). The influence of different air pressures on grain's flying speed has been analyzed with 25μm- diameter grain as the research object that the grain's flying speed increases along with air pressure increases with the maximum speed distributed in 200-250m/s. When the spray gun structure is unchanged, the airflow velocity increases along with air pressure increases and the grain's accelerated speed increases accordingly. The influence of air pressure on grain's speed has been gradually decreased when the pressure is over 0.5MPa. The speed almost has no change in 0.7~0.8MPa. The particle acceleration area is within 0.1 m of the spraying distance. When the spraying distance is between 0.1~0.3m, through fully accelerated, the spraying particle has high flying speed.

Seen from Fig. (**11**), the grain diameter has obvious influence on flying speed of the jet flow particles. Under the precondition to ignore gravity, seen from the formula, the grain's accelerated speed will decrease along with grain diameter increases.

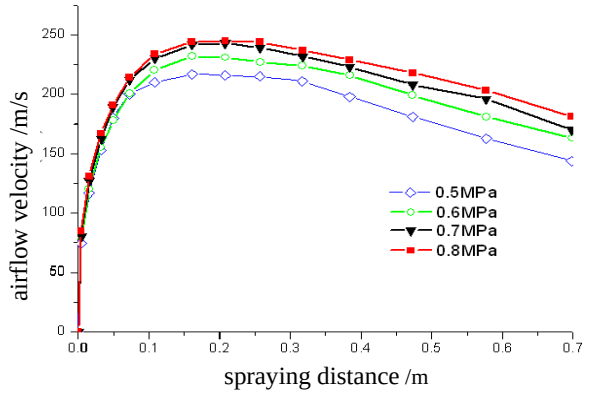

Fig. (10). The effect of different air pressures on airflow velocity.

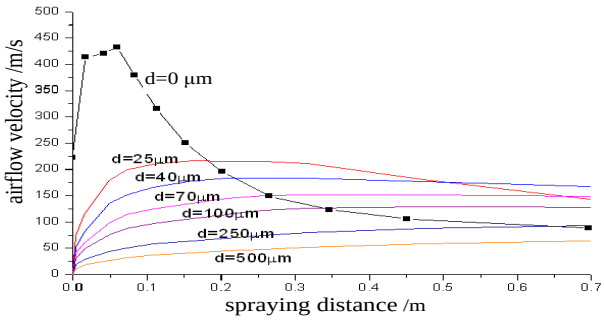

Fig. (11). The effect of different metal grain diameter on airflow velocity.

For the given metal drop, its initial temperature Ti is determined by arc spray gun power and spraying velocity. The overheated liquid molten drop scatters its own heat to the surrounding air through convection and radiation. When liquid cooling is occurred, the molten drop with smaller size even has nucleation or solidification. The molten drop cooling satisfies Newton heat exchange condition. According to Ranz-Marshall relationship, the heat convection coefficient h is expressed as:

$$h = \frac{k_g}{d}\left(2 + 0.6\sqrt{R_e}\cdot\sqrt[3]{P_r}\right) \quad (6)$$

In the formula, k_g is gas thermal conductivity, d is molten drop diameter and Pr is Prandal constant.

Since molten drop has high flying speed, the flying time is relatively short. Additionally, the molten drop has high superheat in arc spraying process, thus, most molten drops will not have solidification at atomization stage. The temperature distribution of molten drop with diameter of d in the atomization process is:

$$\frac{dT}{dt} = \frac{\Delta H_d}{C}\frac{df_s}{dt} - \frac{6h}{d\rho_d C}\left(T - T_g\right) \quad (7)$$

In the formula, T is molten drop temperature, t is flying time, T_g is gas temperature, C is the specific heat of molten drop(WhenT_1 <T< T_0, C= C_1 is the specific heat of liquid phase; when T_s <T≤T_l , C= C_{pd} is the specific heat of solid and liquid mixture; when T≤Ts, C= Cs is the specific heat of solid phase) , ΔH_d is crystallization latent heat in unit mass, $\mathrm{Re} = \frac{\rho v_0 r_0}{\nu}$ is liquidus temperature, ν is solid phase mark. In Schiel equation:

$$f_s = 1 - \left(\frac{T_m - T_l}{T_m - T}\right)^{\frac{1}{1-k_e}} \quad (8)$$

In the formula, T_m is the melting point of pure dissolvent (Fe) and $\frac{v_0^2}{r_0 g}$ is balanced distribution coefficient of solute.

The temperature distribution of grains under different air pressures along with jet flow axis is shown in the Fig. (**12**). In the flying stage, the grain's cooling speed continuously decreases along with grain's temperature decreases and the air velocity has little influence on grain's temperature. However, under the same air pressure spraying condition, grains in different diameters have obvious changes for the temperature, just as shown in the Fig. (**13**). The melting point of stainless steel material 3Cr13 is 1482°C. When the grain temperature in small diameter is lower than the melting point temperature, since the flying speed is unable to reach cold spraying condition (500m/s), the grain is possible not to be deposited for rebounding.

8. THE EXPERIMENTAL RESULTS OF JET FLOW

SprayWatch thermal spraying jet flow inspection device is adopted to detect grain's flying speed and temperature change in the jet flow.

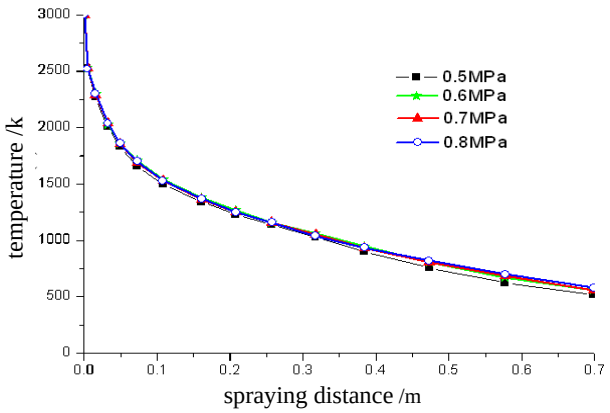

Fig. (12). The temperature distribution of grains under different pressures along with jet flow axis.

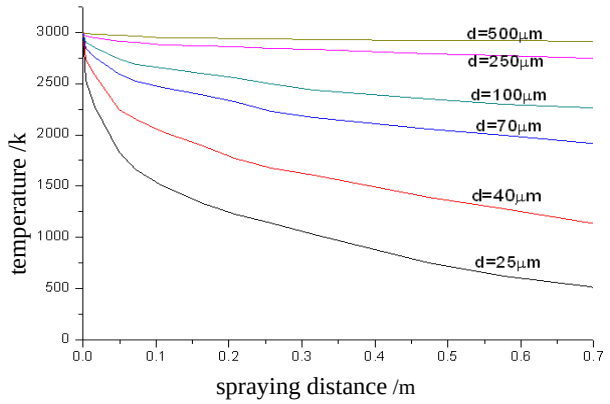

Fig. (13). The temperature distribution of grains under different diameter along with jet flow axis.

SprayWatch is used to measure spraying grain's temperature, speed and flow, etc with CD camera with high speed shutter combined with digital imaging technology, spectrum resolving optics and other technologies. Seen in the Fig. (**14**), SprayWatch monitor spraying jet flow is used to measure grain's speed and temperature in every 30mm along with jet flow axis within the scope of spraying distance of 90-270mm. The experimental result is shown in the Table **6**.

Fig. (14). SprayWatch thermal spraying jet flow inspection device.

Table 6. The Experimental Results of Grain's Speed and Temperature

Spraying Distance (mm)	90	120	150	180	210	240	270
Temperature (K)	2702	2716	2710	2786	2739	2723	2725
Velocity (m/s)	66.73	67.79	70.4	66.85	64.56	63.38	65.61

The jet flow grain speed is 60-70m/s and the jet flow grain temperature is 2700-2800K within the spraying distance scope of 100-300mm. What is unexpected: the grain speed and temperature have little change within the flying distance of 200mm. Seen from Figs. (**15**, **16**), the error between simulation value and the experimental value of jet flow grain is only 5.5% and the error between simulation value and the experimental value of jet flow grain speed is only 14.1%. The matching of speed and temperature testifies the reliability for research result of grain's temperature and speed.

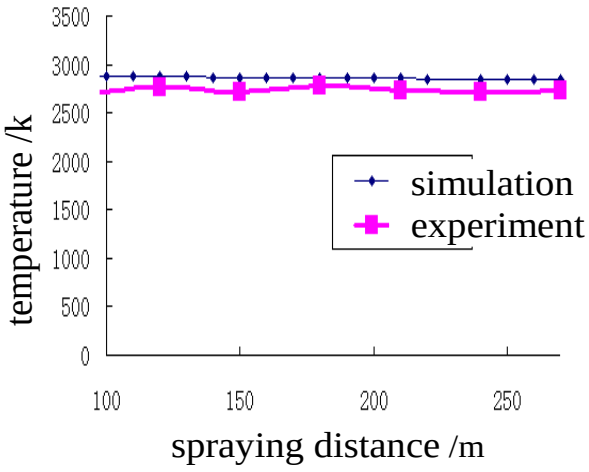

Fig. (15). The temperature compares simulation with experimental value.

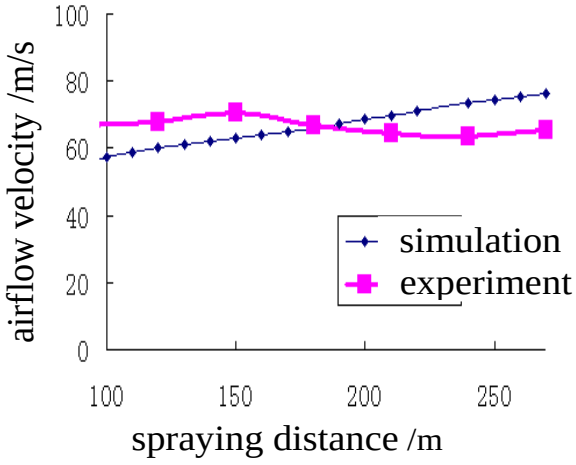

Fig. (16). The airflow velocity compares simulation with experimental value.

9. CONCLUSION

(1) The arc current increases along with arc voltage increases. Under the precondition to guarantee smooth burning of arc, the spraying voltage value should be chosen as low as possible. The voltage for spraying 3Cr13 is confirmed to be 30V in the experiment. When the spraying voltage is unchanged, the spraying current has correspondence relationship with wire feed speed and in the experiment, the spraying current is adjusted through wire feed speed adjustment. The temperature on the coating surface increases along with spraying current increases and the spraying current is confirmed to be 100A in the experiment.

(2) The combined method of numerical simulation and experimental analysis is used to quantitatively analyze for the change process of grain speed and temperature in high-speed flight in the jet flow and jet flow speed and temperature distribution cloud chart. The result showed that, the highest speed of jet flow at the outlet of the spray gun reaches 600m/s; the air velocity quickly reduces to subsonic velocity (about 200m/s) after ejection within the spraying distance of 0-250mm. The air velocity continuously reduces along with the spraying distance increases.

(3) The influence of different air pressures on grain's flying speed is analyzed with grain of 25μm diameter. It is found that the grain's flying speed increases along with air pressure increase with the biggest speed within 200-250m/s and the grain's accelerated speed increases along with increase of air pressure and airflow speed when the spray gun structure is unchanged. Grain diameter has obvious influence on jet flow grain's flying speed. Under the precondition to ignore gravity, the grain's accelerated speed decreases along with grain's diameter increase. In the flying stage, grain's cooling speed is also continuously decreasing along with grain's temperature decrease. The air velocity has little influence on grain's temperature. However, for the grains in different diameters under the same air pressure spraying condition, the temperatures have obvious changes.

ACKNOWLEDGEMENTS

This research was financially supported by the National Natural Science Foundation of China (50875138; 51175276); the Shandong Provincial Natural Science Foundation of China (ZR2009FZ007); Qingdao science and technology program of basic research projects (12-1-4-4-(1)-jch) and the Specialized Construct Fund for Taishan Scholars.

CONFLICT OF INTERESTS

Authors confirm that this article content has no conflicts of interest.

REFERENCES

[1] Jenq-Shyong C, Kwan-Wen C. Bearing load analysis and control of a motorized high speed spindle. Int J Mach Tools Manufacture 2005; 45 (12-13): 1487-93.

[2] Gu RJ, Shillor M, Barber GC, *et al*. Thermal analysis of the grinding process. Math Comput Model 2004; 39 (9-10): 991-1003.

[3] Gviniashvili VK, Woolley NH, Rowe WB. Useful coolant flowrate in grinding. Int J Mach Tools Manufacture 2004; 44 (6): 629-36.

[4] Jin T, Stephenson DJ. Investigation of the heat partitioning in high efficiency deep grinding. Int J Mach Tools Manufacture 2003; 43(11): 1129-34.

[5] Jin T, Rowe WB, McCormack D. Temperatures in deep grinding of finite workpieces. Int J Mach Tools Manufacture 2002; 42 (1): 53-9.

[6] Jin T, Cai GQ. Analytical thermal models of oblique moving heat source plane for deep grinding and cutting. J Manufacture Sci Eng 2001; 123 (2): 185-90.

[7] Lavine AS. An exact solution for surface temperature in down Grinding. Int J Heat Mass Transf 2000; 43 (24): 4447-56.

[8] Lee DS, Choi DH. Reduced weight design of a flexible rotor with ball bearing stiffness characteristics varying with rotational speed and load. J Vib Acoust 2000; 122 (3): 203-8.

[9] Li CH, Hou YL, Ding YC, Cai GQ. Feasibility investigations on compound process: a novel fabrication method for finishing with grinding wheel as restraint. International J Comput Mater Sci Surf Eng 2011; 4 (1): 55 - 68.

[10] Li CH, Hou YL, Liu ZR, Ding YC. Investigation into temperature field of nano-zirconia ceramics precision grinding. Int J Abrasive Technol 2011; 4 (1): 77 - 89.

[11] Li CH, Han ZL, Du C, Ding YC. Numerical study on critical speed modeling of ultra-high speed grinder spindle. Commun Comput Inf Sci 2011; 201 (1): 202-9.

[12] Li C, Hou Y, Chao Du, Ding Y. An Analysis of the Electric Spindle's Dynamic Characteristics of High Speed Grinder. J Adv Manuf Syst 2011; 10 (1): 159-66.

[13] Morgan MN, Jackson AR, Wu H. Optimisation of fluid application in grinding. CIRP Ann Manuf Technol 2008; 57 (1): 363-6.

[14] Moulik PN, Yang HTY, Chandrasekar S. Simulation of thermal stresses due to grinding. Int J Mech Sci 2001; 43 (3): 831-51.

[15] Stephenson DJ, Jin T, Corbett J. High efficiency deep grinding of a low alloy steel with plated CBN wheels. Ann CIRP 2002; 51 (1): 241-4.

[16] Xiu SC, Chao CX, Pei SY. Experimental research on surface integrity with less or non fluid grinding process. Key Eng Mater 2011; 487 (4): 89-93.

[17] Zhu L, Wang W. Modeling and experiment of dynamic performance of the linear rolling guide in turn-milling centre. Adv Sci Lett 2011; 4 (6): 1913-7.

Received: March 4, 2012 Revised: April 25, 2012 Accepted: June 28, 2012